Chirality, Vorticity and Spin Polarization — Experimental Overview

Aihong Tang[1,*]

[1]Brookhaven National Laboratory, Upton NY, USA.

Abstract. In this paper, we provide an exploration of the interrelated topics of chirality, vorticity, and spin polarization in relativistic heavy ion collisions. Our discussion delves into the intricate relationships among these phenomena, examining the recent measurements conducted at both RHIC and LHC. We review the challenges faced, the progress made, and the current state of understanding regarding hot QCD matter under rotation.

1 Introduction

The three subjects, namely chirality, vorticity and spin polarization, are all rooted in the fundamental concept of rotation. A revelation emerged not long ago that in relativistic heavy ion collisions, the system possesses tremendous amount of global angular momentum [1], alongside an immensely powerful electromagnetic field [2], generated as two nuclei pass by each other in close-to-light speed. While a fraction of this angular momentum is carried away by spectator nucleons, a small portion is deposited in the interaction region in the form of vorticity fields. These vorticity fields give rise to localized vorticity, which, through spin-orbital coupling, exerts its influence on particle spins. Consequently, a system-wide particle polarization, known as global polarization, occurs (see reviews [3, 4] and references therein). Additionally, the robust magnetic field sets the stage for a remarkable QCD phenomenon — the Chiral Magnetic Effect (CME) [5]. These themes have captivated the scientific community in recent years, sparking intensive interest and ongoing explorations in this field.

2 Global polarization

The study of global polarization is facilitated through the analysis of polarization in hyperons like Λ's. Λ decay is a parity-violating weak decay and the proton tends to go off in the direction of Λ spin. In addition, the polarization of the Λ hyperon is carried solely by the strange quark. Thus, investigating the polarization of Λ hyperons provides valuable insights into the polarization of s-quarks. In practice, the Λ polarization parameter, denoted as P_H, is determined by fitting the distribution of the angle (θ^*) — measured in Λ's rest frame — between the proton momentum and the polarization axis. The distribution is described as $\frac{dN}{d\Omega^*} = \frac{1}{4\pi}(1 + \alpha_{\rm H} {\rm P_H} {\rm cos}\theta^*)$, where $\alpha_{\rm H}$ is the decay parameter for Λ, and P_H signifies the polarization of Λ.

The STAR experiment at RHIC has reported significant global polarization in Λ hyperons as a function of collision energy [6]. Initially, this trend was attributed to the presence of thermal vorticity [7]. At higher energies, the fireball at middle rapidities

*e-mail: aihong@bnl.gov

exhibits characteristics of a boost-invariant fluid, resulting in small vorticity and consequently, a small P_H. However, as more data emerged, discrepancies arose. One challenge surfaced in the measurement of global polarization concerning the azimuthal angle relative to the reaction plane. The data indicated that P_H was strongest in the in-plane direction and diminished out-of-plane (depicted as P^J in Fig. 1(a)). Another complexity arose in measuring polarization along the beam direction (z-axis) concerning azimuthal angle (P^z in Fig. 1(c)). These measurements revealed intricate substructures within the vorticity field. Specifically, the global vorticity field appeared strongest in-plane, and the local vorticity field along the beam direction is consistent with a robust elliptic flow expansion along the in-plane direction. The existing framework at that time, primarily considering thermal vorticity, failed to predict the observed trend for both measurements, leading to a "sign puzzle". This enigma prompted the community to explore additional mechanisms potentially overlooked. Recently, we recognized that incorporating other contributions, particularly from thermal shear, could rectify the sign puzzle. The inclusion of thermal shear, which is akin to thermal vorticity but characterized by the symmetric gradient of the four-temperature, allowed for right predictions (Fig. 1(b) and Fig. 1(d)) aligning with the observed trend in the data.

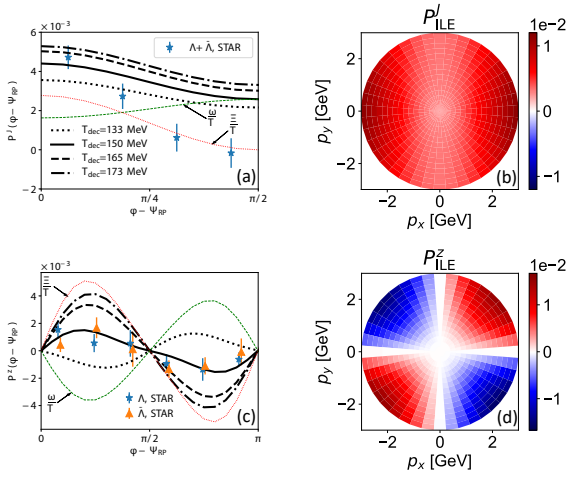

Figure 1: Left column : The global polarization [8] (a) and local polarization in beam direction [9] (c) as a function of azimuthal angle. The contribution from thermal vorticity ($\frac{\omega}{T}$) and thermal shear ($\frac{\Xi}{T}$) are indicated as green and red dotted lines, respectively. Right column : the theoretical calculations [10] of the corresponding polarization as a function of its transverse momentum (p_x, p_y), with the contribution from thermal shear included.

However, this agreement arises from the delicate balance between thermal vorticity and thermal shear, both making substantial contributions but in opposite directions. Even a minor alteration in either of these contributions could significantly impact the results. Throughout this process, we also observed the sensitivity of the outcomes to several other variables. For instance, in the theoretical calculations depicted in Fig. 1, altering the deconfinement temperature led to significant changes in the results. Additionally, understanding aspects such as why T-vorticity follows the correct trend [11] and grasping the significance of the *s*-quark memory scenario explaining the data trend [12], etc., are ongoing challenges. Mastering the control of these factors to ensure stability and robustness in our predictions remains a active pursuit within the community.

The collective polarization pattern serves as a valuable tool for exploring the properties of the hot dense matter formed in relativistic heavy ion collisions. For instance, varying the system size allows one to examine how the global polarization responds to the change in vorticity profile in difference systems. The expectation is that larger systems maintain better boost invariance at middle rapidities, leading to reduced vorticity and, consequently, smaller global polarization. The STAR experiment examined global polarization for Λ particles in ${}^{96}_{44}$Ru +${}^{96}_{44}$ Ru and ${}^{96}_{40}$Zr +${}^{96}_{40}$ Zr collisions [13], and compared it to that in ${}^{197}_{79}$Au +${}^{197}_{79}$ Au collisions (Fig. 2(a)). Surprisingly, despite a roughly twofold

difference in the number of nucleons between $^{197}_{79}$Au and $^{96}_{44}$Ru (or $^{96}_{40}$Zr) ions, no significant distinctions were observed within the margin of error. While the measurement's uncertainty is notable, this observation prompts for further contemplation and analysis.

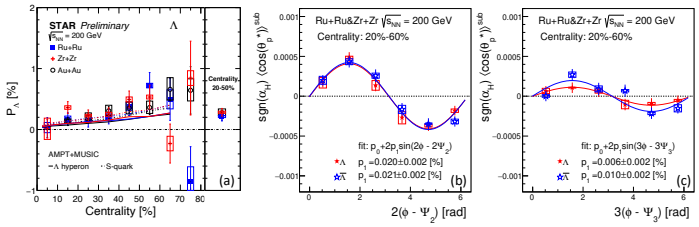

Figure 2: (a) Global polarization of Λ hyperon as a function of centrality in $^{197}_{79}$Au +$^{197}_{79}$ Au, $^{96}_{44}$Ru +$^{96}_{44}$ Ru and $^{96}_{40}$Zr +$^{96}_{40}$ Zr collisions at $\sqrt{s_{NN}}$ = 200 GeV [13]. (b) and (c) : Λ and $\bar{\Lambda}$ polarization along the beam-axis as a function of azimuthal angle with respect to second (b) and third (c) order event plane [14].

One can also examine the fine structure of the vorticity by studying the polarization pattern along the beam axis as a function of angle with respect to the second and third order event plane. Extensive statistical data from isobar collisions were analyzed [14], revealing modulations depicted in Fig. 2(b) and Fig. 2(c). Remarkable, both measurements exhibit similar modulations. This observation aligns with hydrodynamic calculations incorporating thermal vorticity and shear contributions, indicating the presence of rich local vorticity structures generated by flow expansions.

3 Global spin alignment

The collective spin phenomena can also be studied with vector mesons. For vector mesons with spin-1, like ϕ and K^{*0}, the spin state can be described by a 3x3 spin density matrix, and the diagonal element ρ_{00} corresponds to the probability of finding a vector meson in spin state 0 out of 3 possible spin states of -1, 0 and 1. If there is no spin alignment, ρ_{00} is 1/3, otherwise, ρ_{00} deviates from this value. The determination of ρ_{00} from data is similar to the hyperon spin polarization analysis, except that, the distribution of the angle of a daughter and the quantization axis in meson's rest frame is fitted with an even function instead of an odd one : $\frac{dN}{d(\cos\theta^*)} \propto (1-\rho_{00}) + (3\rho_{00}-1)\cos^2\theta^*$.

The STAR experiment reported measurements of ρ_{00} for ϕ and K^{*0} as a function of collision energy [15]. Surprisingly, the ϕ-meson exhibits significant global spin alignment, while K^{*0}-meson shows little alignment (Fig. 3). This observation is intriguing as the global spin alignment for ϕ-meson was thought to result from multiple sources, including the quark coalescence with vorticity and magnetic field, the contribution from electric component of vorticity tensor, the classic electric field contribution, and the fragmentation. However, these conventional contributions are at the 10^{-4} or 10^{-5} level, insufficient to explain the data. Additional sources like local spin alignment and turbulent color fields negatively affect ρ_{00}. This suggests new mechanisms at play in the substantial ρ_{00} for ϕ-mesons. Two models have been proposed recently: one involves local fluctuation of the strong force field of vector mesons, and the other involves fluctuations of the glasma fields. These models may explain the ob-

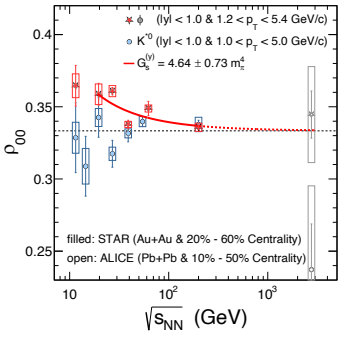

Figure 3: Global spin alignment of ϕ and K^{*0} as a function of collision energy [15]. The red solid curve represents the fit to ϕ data using a model based on ϕ-meson strong force field.

served large signal. Notably, the contribution from the vector meson's strong force field can explain the magnitude and, to some extent, the energy dependence(see ref. [16] and references therein). This observation underscores the pivotal role of the strong force field in influencing quark spin and demonstrates that ρ_{00} is sensitive to local field fluctuations, in contrast to hyperon polarization, which is sensitive to its mean value.

One specific reason why the theory can calculate the ρ_{00} for ϕ-meson is because the two quarks that constitute the ϕ-meson are from the same flavor family. This also makes the ρ_{00} of J/ψ an interesting measurement, as it consists of c and $\bar{c}$, which are from the same flavor family as well. Both ALICE and STAR (not shown) have conducted the measurement. In Fig. 4, the ρ_{00} is presented as a function of transverse momentum and plotted with the newly measured prompt D^{*+} meson. The J/ψ displays ρ_{00} that is less than 1/3 at low p_T, while the D^{*+} meson exhibits value larger than 1/3, both seemingly increasing with p_T. More theoretical guidance is needed to understand these results.

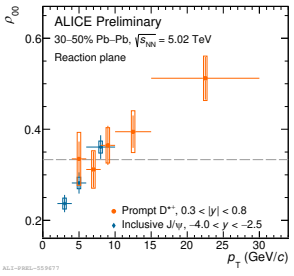

Figure 4: ρ_{00} measured as a function of transverse momentum for J/ψ and D^{*+} [17].

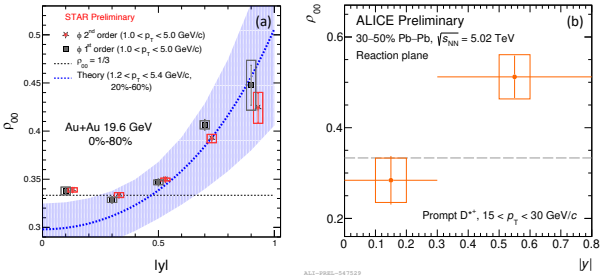

Figure 5: Rapidity dependenc of ρ_{00} measured by STAR [18] and ALICE [17].

STAR and ALICE also reported the rapidity dependence of ρ_{00} for ϕ and D^{*+}-meson, respectively (Fig. 5). Both measurements indicate a strong increase in ρ_{00} with rapidity. The STAR measurement is compared to theoretical prediction based on the strong force field, and the trend is found to be consistent. According to this specific theory, the trend arises from the fact that fluctuations are more prominent in the direction perpendicular to the motion.

4 Directed flow splitting due to electromagnetic field

Despite the widespread anticipation of an ultra-strong magnetic field in non-central heavy ion collisions, the evidence of its impact on the QGP has remained elusive. However, recent studies by the STAR experiment have explored the splitting in directed flow between positively and negatively charged particles across different centralities. It was observed (Fig. 6) that the $\Delta(dv_1/dy)$ for (anti)protons and kaons changed sign when transitioning from peripheral to central collisions, a phenomenon not observed in pions. This observed pattern aligns with the presence of a potent electromagnetic field, where Faraday and Coulomb effects dominate over the Hall effect for light hadrons.

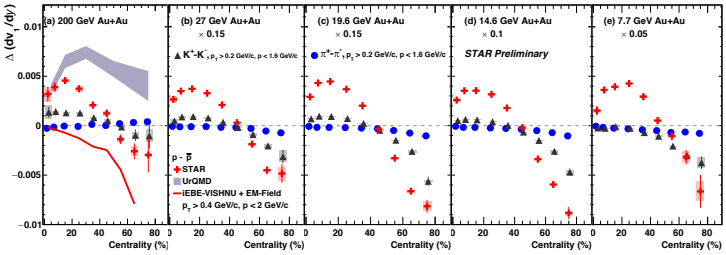

Figure 6. Directed flow splitting, $\Delta(dv_1/dy)$ for light hadrons as a function of centrality [19].

5 Chiral Magnetic Effect

The presence of a strong magnetic field enables the occurrence of the chiral magnetic effect [5]. CME initiates from a local imbalance of chiral charge within the QCD vacuum. In the presence of an external magnetic field, this imbalance leads to the separation of positively and negatively charged particles along the magnetic field direction. This separation is usually quantified through the observable $\Delta\gamma \equiv \gamma_{\mathrm{OppositeSign}} - \gamma_{\mathrm{SameSign}}$, where the γ represents the azimuthal correlation between two particles, α and β, and the reaction plane ψ_{RP}, defined as $\gamma \equiv \langle\cos(\phi_\alpha + \phi_\beta - 2\psi_{RP})\rangle$. However, several non-CME related backgrounds, primarily driven by local charge conservation and the elliptic flow of resonance, can mimic the $\Delta\gamma$ signal. Addressing these challenges, RHIC conducted an isobar program wherein two isobars, $^{96}_{44}$Ru and $^{96}_{40}$Zr, have the same number of nucleons (resulting in similar backgrounds) but different protons, leading to different magnetic fields and CME strengths. An initial blind analysis faced complications due to the non-identical multiplicities of the two isobar systems. To overcome these complexities, the STAR experiment re-analysed the isobar collisions with post blind analyses. The updated baseline plot (Fig. 7) was obtained, with an upper limit for the CME fraction set at ~10% at a 95% confidence level. Utilizing a forced match technique, designed to reconcile the multiplicities of the two isobar systems through re-weighting, the ratio of CME observables ($\Delta\gamma$ and the Signed Balance Function) was found to be remarkably consistent with unity.

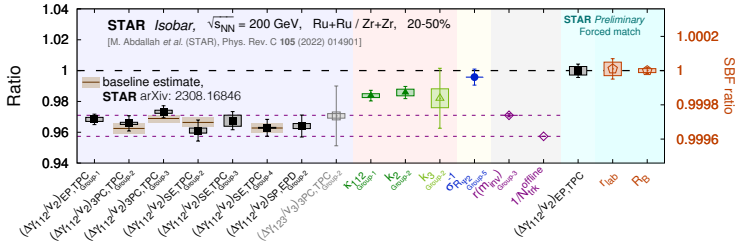

Figure 7. Status of post-blinding analyses of CEM search in isobar collisions [20].

The CME search with isobar collisions, relying on the ratio between the two isobar systems, is entirely dependent on the disparity in signal strength between these systems, which might not be as pronounced as initially expected. The absence of a notable difference in CME strength between the two isobar systems does not necessarily negate the existence of CME. The STAR experiment continued to pursue the CME search within individual systems using the Event Shape Selection (ESS) technique. This approach involved an enhanced event shape selection based on pair q^2 (in contrast to the previously used single particle q^2) combined with single particle v_2. The left data-group in Fig. 8 displays the results obtained with ESS, represented by solid blue circles. Open circles serve as a consistency check for an observable solely sensitive to backgrounds. This study hints at a potential signal excess above the baseline. The right group in Fig. 8 presents result obtained through the usual Event Shape Engineering, employing particles of interest and particles for event shape categorization from two distinct kinematic regions. It shows an excess of ~1 σ above baseline.

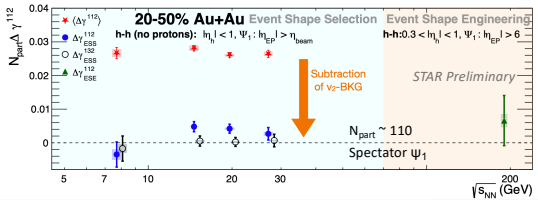

Figure 8: Search for CME with Event Shape Selection and Event Shape Engineering [21].

Traditionally, resonance v_2 has been considered a mere background in CME analyses. However, recent research reveals that v_2 itself can be influenced by genuine CME signals

(Fig. 9(a)). Intriguingly, this phenomenon extends to ρ_{00} as well. It has been noted that a deviation of ρ_{00} from the expected 1/3 value for vector mesons, particularly ρ mesons, can introduce a finite "signal" to CME observables, creating a background effect for CME. Surprisingly, it has been observed (Fig. 9(b)) that the ρ_{00} of vector mesons can itself be affected by genuine CME signals, alongside other mechanisms altering ρ_{00}. This dual influence, where the CME impacts both v_2 and ρ_{00}, while v_2 and ρ_{00} can also mimic CME, raises the fundamental question of distinguishing between signal and background — determining what is the cause and what is the consequence.

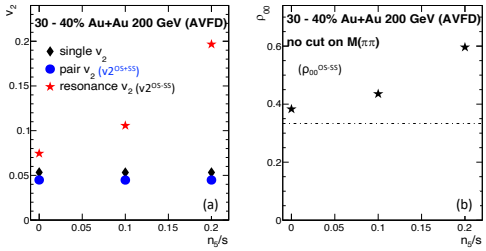

Figure 9. The variation of v_2 [22] and ρ_{00} [23] as a function of CME strength, indicated by chirality charge density n_5/s. Here, the distinction between opposite and same sign pairs is denoted as "resonance", a convenient categorization without sacrificing generality.

6 Conclusion

Our exploration of the rotational dynamics within the strongly interacting Quark Gluon Plasma (QGP) has revealed complex and enigmatic phenomena. Our understanding of these intricacies is still developing. However, investigating the interplay of the QGP with rotation and the influence of a potent magnetic field has unveiled a promising realm for research. Its potential is yet to be fully explored, presenting an exciting frontier for future studies.

References

[1] Z.T. Liang, X.N. Wang, Phys. Rev. Lett. **94**, 102301 (2005), [Erratum: Phys.Rev.Lett. 96, 039901 (2006)], nucl-th/0410079

[2] D.E. Kharzeev, L.D. McLerran, H.J. Warringa, Nucl. Phys. A **803**, 227 (2008), 0711.0950

[3] F. Becattini, J. Liao, M. Lisa, Lect. Notes Phys. **987**, 1 (2021), 2102.00933

[4] F. Becattini, Rept. Prog. Phys. **85**, 122301 (2022), 2204.01144

[5] D. Kharzeev, R.D. Pisarski, M.H.G. Tytgat, Phys. Rev. Lett. **81**, 512 (1998), hep-ph/9804221

[6] L. Adamczyk et al. (STAR), Nature **548**, 62 (2017), 1701.06657

[7] F. Becattini, I. Karpenko, M. Lisa, I. Upsal, S. Voloshin, Phys. Rev. C **95**, 054902 (2017), 1610.02506

[8] T. Niida (STAR), Nucl. Phys. A **982**, 511 (2019), 1808.10482

[9] J. Adam et al. (STAR), Phys. Rev. Lett. **123**, 132301 (2019), 1905.11917

[10] F. Becattini, M. Buzzegoli, G. Inghirami, I. Karpenko, A. Palermo, Phys. Rev. Lett. **127**, 272302 (2021), 2103.14621

[11] H.Z. Wu, L.G. Pang, X.G. Huang, Q. Wang, Phys. Rev. Research. **1**, 033058 (2019), 1906.09385

[12] B. Fu, S.Y.F. Liu, L. Pang, H. Song, Y. Yin, Phys. Rev. Lett. **127**, 142301 (2021), 2103.10403

[13] X. Gou for STAR, Quark Matter 2023

[14] A. M.I. et al. (STAR) (2023), 2303.09074

[15] M.S. Abdallah et al. (STAR), Nature **614**, 244 (2023), 2204.02302

[16] X.L. Sheng, L. Oliva, Z.T. Liang, Q. Wang, X.N. Wang, Phys. Rev. Lett. **131**, 042304 (2023), 2205.15689

[17] L. Micheletti for ALICE, Quark Matter 2023

[18] G. Wilks for STAR, Quark Matter 2023

[19] A. P. Dash for STAR, Quark Matter 2023

[20] Y. Feng for STAR, Quark Matter 2023

[21] Z. Xu for STAR, Quark Matter 2023

[22] Z. Xu, B. Chan, G. Wang, A. Tang, H.Z. Huang (2023), 2307.14997

[23] D. Shen, J. Chen, A. Tang and G. Wang, Quark Matter 2023